Infrared absorption study of Fermi resonance and hydrogen-bond symmetrization of ice up to 141 GPa

M. Song
Core Research for Evolutional Science and Technology, Japan Science and Technology Corporation, Kawaguchi, Saitama 332-0012, Japan

H. Yamawaki, H. Fujihisa, M. Sakashita, and K. Aoki*
National Institute of Materials and Chemical Research, 1-1 Higashi, Tsukuba, Ibaraki 305-8565, Japan and Core Research for Evolutional Science and Technology, Japan Science and Technology Corporation, Kawaguchi, Saitama 332-0012, Japan

(Received 8 July 1998; revised manuscript received 7 April 1999)

The infrared absorption spectra of H_2O and D_2O ices were measured with a diamond-anvil cell up to 141 GPa at 298 K. The high-pressure spectra corrected for diamond absorption provided the substantial absorption profile of ices over the whole pressure range measured. A sequence of pressure-induced Fermi resonance was observed between the softening stretch mode and the combinations of rotational and bending modes below 55 GPa as reported previously. One rotational mode showed an abrupt increase in the peak frequency at 58 ± 3 GPa in H_2O ice and 68 ± 3 GPa in D_2O ice. This can be attributed to a transition from ice VII to proton-tunneling-disordered ice VII. A further transition into proton-disordered ice X was inferred from the spectral change to occur roughly at 65–75 GPa for H_2O and 80–90 GPa for D_2O. [S0163-1829(99)04133-8]

INTRODUCTION

The property of ice under high compression, which can provide crucial insights into pressure-induced molecular dissociation, the evolution of chemical bonding, and the quantum effects of hydrogen such as tunneling, has attracted considerable theoretical and experimental interest in the last couple of decades. Ice is a prototype of hydrogen-bonded molecular solids, showing very rich behavior in the pressure-temperature phase diagram. At pressures above 2 GPa, however, there exist only two known molecular phases, ice VII ($Pn3m$) and VIII ($I4_1/amd$), which possess a body-centered-cubic (bcc) and a slightly distorted bcc sublattice of oxygen atoms, respectively.[1,2] At room temperature ice VII maintains the bcc sublattice at least up to 128 GPa while the oxygen-oxygen distance $r_{O\text{-}O}$ decreases to 0.223 nm.[3] This $r_{O\text{-}O}$ value is well shorter than a predicted symmetrization distance ranging from 0.23 to 0.25 nm.[4–7] It has been inferred that the protons already reach the midpoints between two neighboring oxygen atoms in ice VII at such high pressures; a hydrogen-bond symmetric phase (ice X) would be formed as predicted by Holzapfel.[4]

X-ray and neutron powder diffraction and infrared (IR) absorption measurements have been made to probe a transition into the symmetric phase of ice. A detailed examination of the equation of state of ice lead to an anomaly at 66–70 GPa,[8,9] indicating an occurrence of second- or higher-order phase transition probably related to the hydrogen bond symmetrization. Neutron-diffraction measurement, which is capable of probing H (or D) position, was made to a limited pressure of 20 GPa.[10–12] The O-D covalent bond length $r_{O\text{-}D}$ in D_2O ice increases slightly with pressure to 10 GPa, showing a trend toward symmetrization on further compression. IR spectra provided more clearly an evidence for the symmetrization. Appearance of two absorption peaks above 100 GPa after disappearance of the molecular vibrational peaks in H_2O ice was definitely interpreted as a transition from ice VII to symmetric ice X, which likely takes place around 60 GPa.[13,14] However, the pressure behavior of the OH stretching mode, which was expected to play a key role in detection of the hydrogen-bond symmetrization, was not precisely investigated owing to interference by vibrational mode coupling or Fermi resonance.[15,16] Tunnel splitting of the vibrational states in association with the symmetrization process[17] was another factor making the interpretation of the high-pressure spectra much more complicated.

Theoretical investigations using semiempirical methods, molecular-dynamics simulations, and *ab initio* quantum-mechanical methods have been carried out to obtain the microscopic view of symmetrization mechanism and to estimate the phase-transition pressure.[6,7,18–20] The results predicted a softening behavior of the OH stretching mode and a strong anharmonicity toward the hydrogen-bond symmetrization as intuitively speculated from a continuous deformation of the hydrogen bond potential from a double- to single-well shape. A suggestive picture was proposed to the symmetrization process from *ab initio* quantum-mechanical calculations, displaying dramatic changes in proton distribution in a virtual ice at 100 K in association with sequential transformations: ice VIII→translational-proton-tunneling-disordered ice VII→proton-disordered ice X→proton-ordered ice X.[18] The transitions were shown to be dominated by quantum-mechanical effects such as the tunneling and the zero-point motions of protons. Translational-proton-disordered ice VII (hereafter referred as disordered VII) is characterized as a bimodal proton distribution arising from the enhanced proton tunneling along a double-well potential with a depressed central barrier, whereas proton-disordered ice X (disordered X) as a unimodal distribution of the proton

 ©1999 The American Physical Society

with a zero-point motion energy exceeding the underlying potential barrier. In proton-ordered ice X, a harmonic single-well potential is realized, resulting in a unimodal narrow proton distribution along it.[6,18] The energy levels of the proton vibrations in a potential being deformed from a double to a single minimum shape have been investigated using a generalized double Morse potential.[19] The calculated tunnel splitting energies and their pressure variations would be of great use to interpret the vibrational spectra of ice measured at high pressures especially near the hydrogen bond symmetrization.

IR measurement with a diamond-anvil cell (DAC) is at present time a promising tool to investigate the hydrogen-bond symmetrization in ice at pressures beyond 100 GPa. Diamond exhibits strong IR absorption in a frequency region 1800–2400 cm^{-1}, which is a critical span for monitoring the softening behavior of O-H (D) stretching modes. An intense synchrotron infrared source and thin diamond anvils have been used in IR reflectivity measurements to reduce interference of the diamond absorption on ice spectra.[16] However, in all the previous IR measurements the spectrum of an empty DAC at ambient pressure was employed as a reference spectrum to remove the diamond absorption.[13–16] The spectral change of diamond absorption with pressure was not taken into account. Such an absorption correction should have injured the substantial feature of ice spectra measured at very high pressure. In addition, it has been pointed out that highly strained diamonds might give rise to an IR activity of the optical phonon which is inactive at ambient condition and also that an IR-active mode of KBr would develop its absorption to a region of 700–1100 cm^{-1} at pressures of 100–150 GPa.[19] Therefore, a measurement of reliable and qualified IR spectra of ice free from these disturbances has been required to clarify the hydrogen bond symmetrization process.

We present IR absorption spectra of H_2O and D_2O ices measured with a DAC up to 120 and 141 GPa, respectively, at 298 K. The spectra were finely corrected for diamond absorption using the spectra of a KBr-filled DAC measured over a wide pressure range to 135 GPa. By contrast to H_2O ices, no IR spectral data has been reported for D_2O ice yet. The substantial spectra of ice obtained by an appropriate absorption correction have allowed a quantitative comparison with the calculated results on the proton vibrational state and hence a deep understanding of the hydrogen-bond symmetrization process.

EXPERIMENTAL PROCEDURE

IR spectra of ices were measured at 298 K and pressures up to 141 GPa. Distilled H_2O water and high-purity D_2O (99.996%, Aldrich) were used. High pressures were generated using a DAC with type-II-A diamond anvils. Pairs of 1.5 mm and 2.1 mm thick diamond anvils were employed for a high-pressure measurement below and above 55 GPa, respectively. Hardened stainless-steel and rhenium metal were used as gasket materials. Both of them were capable of confining the sample in a gasket hole at pressures above 100 GPa. Since the fundamental vibrational bands of ice exhibit very strong absorption, a thin film roughly less than 1 μm in thickness was required to avoid saturation of the absorption peaks.[13,15] Ruby chips and KBr grains were pushed together into a sample chamber made in the metal gasket which was fixed on the culet of a piston diamond anvil. Pressure medium KBr is transparent for the measuring IR range 500–6700 cm^{-1}, not giving rise to disturbance in ice spectra. Ice film was prepared by condensing evaporated water on a flattened top surface of KBr pressure medium filling almost the whole space of the sample chamber. Ice film thus prepared was squeezed together with KBr pressure medium and ruby chips in a sandwich configuration between the diamond anvils. The sample preparation was carried out in a nitrogen-gas purged glove box.

The absorption spectra of ices were acquired at a 4 cm^{-1} spectral resolution with a Fourier-transform-infrared spectrometer over the wave-number region of 500–6700 cm^{-1}. For the measurement below 55 GPa, the initial size of the sample chamber was 100 μm in diameter and about 60 μm in height and the measuring area was trimmed off into a 45 μm$\times$45 μm square with an adjustable optical mask. For the measurement beyond 55 GPa, the chamber size and the measuring area were reduced to 30 μm in diameter and 25 μm in height and a 25 μm$\times$25 μm square, respectively. The pressure was determined by ruby-fluorescence measurement on the basis of a quasihyrostatic ruby scale.[21]

The spectra of a KBr-filled DAC were measured at various pressures up to 135 GPa to obtain the reference spectra used for an appropriate correction of diamond and KBr absorption. Two experiments were made: one with 1.5-mm-thick diamond anvils up to 55 GPa and another with 2.1-mm-thick anvils up to 135 GPa. Typical spectra of the KBr-filled cell are shown in Fig. 1(A). The upper two spectra show the absorption spectra measured with the 1.5 mm diamond anvils. The spectrum at 23.4 GPa is nearly identical to that measured at 50.1 GPa. The lower two spectra are those measured with the 2.1 mm diamond anvils at higher pressures. The IR absorption peaks are obviously taller than those measured with the 1.5 mm diamond anvils, reflecting an increase by 40% in anvil thickness. They are almost saturated at the peak. No significant difference is observed between the spectra measured at 52.2 and 135 GPa in spite of a wide pressure interval of 83 GPa. There is neither an absorption peak of diamond developed with the breaking of an IR inactivity of its optical, nor an absorption peak of KBr predicted to move to a frequency range 700–1000 cm^{-1} at pressures above 100 GPa.[19]

We examined more carefully the influence of absorption correction on the ice spectra. An example of the correction is given in Fig. 1(B). Spectra *a* and *b* are those of H_2O ice at 53.3 GPa obtained after absorption correction using an ambient-pressure spectrum of an empty DAC and 50.1-GPa spectrum of the KBr-filled DAC, respectively. Marked differences can be seen in the region 1800–3000 cm^{-1}. The peaks indicated by arrows in spectrum *a* are artificially produced by an inappropriate correction using the ambient-pressure spectrum, while they all are wiped out in spectrum *b* corrected with the 50.1-GPa spectrum of the KBr-filled cell. The spectra measured with the 1.5-mm diamond anvils are thus satisfactorily corrected for the diamond absorption. Spectrum *c* is obtained by dividing the absorption spectrum of the KBr-filled DAC at 50.1 GPa by that of the empty DAC at ambient pressure. It demonstrates clearly that the

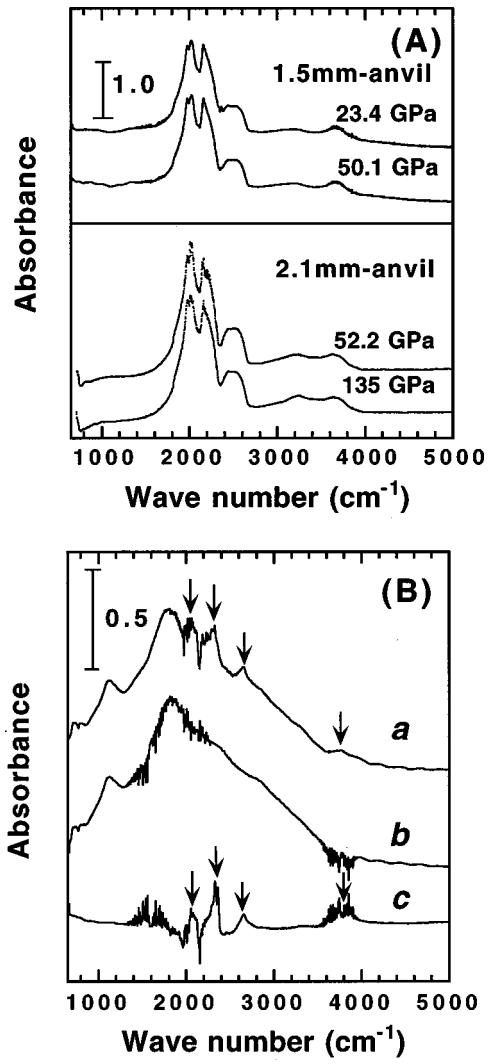

FIG. 1. (A) IR spectra of KBr-filled diamond anvil cells. The spectra at 23.4 and 50.1 GPa were measured with 1.5 mm-thick anvils and those at 52.2 and 135 GPa with 2.1 mm-thick anvils. All the peaks observed are due to diamond absorption, showing a very slight change in peak shape and intensity with pressure. (B) An example of absorption correction. Spectrum *a* and *b* are those of H_2O ice at 53.3 GPa after correction using spectra of the empty DAC at ambient pressure and KBr-filled DAC at 50.1 GPa, respectively. Spectrum *c* is that of a KBr-filled DAC at 50.1 GPa corrected with the ambient pressure spectrum. The structures at 2100, 2300, 2700, and 3750 cm^{-1} in spectrum *a* (indicated with arrows) are shown to arise from inappropriate absorption correction using the ambient pressure spectrum.

structures marked by arrows in spectrum *a* are attributed to the pressure change in diamond.

The high-pressure correction is only slightly effective for the IR spectra measured with the 2.1-mm diamond anvils. A pair of 2.1-mm diamonds transmits a few percent of incident infrared lights in the diamond absorption region. This value is less than one-fifth of the transmittance for the 1.5-mm diamond anvils, being too small to allow a satisfactory correction of the diamond absorption. The IR spectra of the KBr-filled DAC with the 2.1-mm diamond anvils were measured up to 135 GPa at an appropriate pressure interval and used for the diamond absorption correction. This correction, however, leaves some structures in the region 1800–2400 cm^{-1} due to an incomplete subtraction of the diamond absorption modified intensively by high compression. However, the purpose of the measurements above 55 GPa was focused on investigation of the dominant spectral change in association with the hydrogen-bond symmetrization, which was expected to be detected in the region below 1800 cm^{-1}. The incomplete absorption correction hence has made no serious interference for this measurement.

RESULTS AND DISCUSSION

IR spectra were measured for H_2O and D_2O ices at 298 K and pressures from 2 to 141 GPa. At room temperature, it is known that water freezes at 0.7 GPa into ice VI with an orthorhombic structure and then transforms into ice VII with a cubic structure at 2.0 GPa. In our experiments, an ice film was prepared in the DAC at low temperature around 250 K and confined by squeezing it in the cell to a few GPa. The pressure was held above 2 GPa, while the DAC was warmed up to room temperature. We hence started IR measurements from ice VII. Two experimental runs were made for H_2O and D_2O ices; in the first run, the 1.5-mm-thick anvils were used to obtain the detailed spectral features of the molecular vibrations up to about 55 GPa, and in the second run the 2.1-mm-thick anvils were employed to generate higher pressures beyond 55 GPa and to investigate a phase transition into symmetric ice.

A. Vibrational mode assignment of ice VII

The disordering in molecular orientation in ice VII destroys a normal selection rule for IR absorption, making it hard to assign distinctly the observed peaks to the possible vibrational modes. However, the similarity of the spectra of ice VII and VIII, which have the same short-range order in molecular arrangement and can be converted to each other by introducing slight distortion of the primitive cells, allows a reasonable peak assignment for ice VII based on that for ice VIII (point group D_{4h}) as reported in the previous papers.[22,23] Here we follow the same procedure in assignment of the IR vibrational peaks of ice VII.

Figure 2 shows three infrared spectra of H_2O-ice VII measured at a pressure interval of roughly 10 GPa with the vibrational modes assigned. The O-H stretching peaks at about 3100 cm^{-1} in a 12.5-GPa spectrum show an asymmetry peak shape, which can be deconvoluted into the asymmetric $\nu_3(E_u)$ and symmetric stretching vibration $\nu_1(A_{2u})$.[22,23] In the low-frequency region below 1000 cm^{-1}, there is a strong absorption peak of a rotational mode $\nu_R(E_u)$. It is accompanied by a shoulder peak in the high-frequency side, which is tentatively assigned to another rotational mode $\nu_{R'}(E_u)$ according to the peak assignment of ice VIII.[24] An absorption shoulder, appearing at the low-frequency side of the $\nu_R(E_u)$ peak in a 30.1-GPa spectrum, can be assigned to the translational vibration $\nu_T(E_u)$. The peak of the OH bending vibration $\nu_2(A_{2u})$ is located steadily at about 1600 cm^{-1}. The overtones and combinations of the fundamental modes are assigned by manipulating the fundamental peak frequencies measured at various pressures in this study. In the order of decreasing frequency, they are $\nu_2(A_{2u})+\nu_R(E_u)$, $2\nu_{R'}(E_u)$, and $2\nu_R(E_u)$ as described in the spectra. The absorption

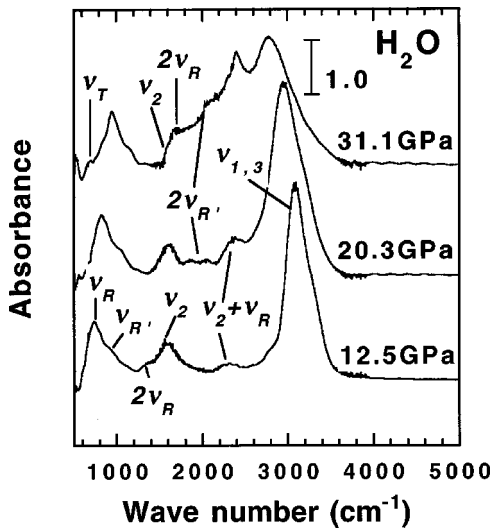

FIG. 2. Vibrational mode assignment of the IR absorption peaks of H_2O ice VII. $\nu_{1,3}$ is the symmetric and asymmetric stretching vibrations; ν_2 is the bending vibration; ν_R is the rotational vibration; $\nu_{R'}$ is the high-frequency component of rotational mode; ν_T is the lattice translational vibration.

spectra of D_2O-ice VII show pressure changes very similar to those of H_2O ice and the observed peaks are interpreted by following the same procedure applied to H_2O ice.

B. Fermi resonance

The spectra of H_2O and D_2O ices up to 55 GPa are depicted in Figs. 3(A) and 3(B). Each fundamental mode shows characteristic pressure behavior. In H_2O ice, the $\nu_{1,3}$ stretching peaks shift to low frequency; the ν_2 bending peak stays almost at the same position; the $\nu_{R,R'}$ rotational peaks move to high frequency. The spectral profile changes more rapidly above 20 GPa. This is due to peak broadening by increased anharmonicity especially for the $\nu_{1,3}$ peaks and coupling of the vibrational modes again through anharmonicity. As shown in Fig. 3(B), D_2O ice exhibits spectral changes in a manner very similar to those of H_2O ice.

Figures 4(A) and 4(B) show the frequency variations of the absorption peaks with pressure obtained for H_2O and D_2O ices, respectively. The peak frequencies measured by the high-pressure experiment beyond 55 GPa are plotted together. It is unusual that the frequencies vary with pressure not monotonically. The $\nu_{1,3}$ stretching frequency, for instance, which shows a rapid and monotonic decrease from 3500 cm^{-1} at ambient pressure, avoid a crossing with the $\nu_2+\nu_R$ frequency rising up from 2200 cm^{-1}. A repulsive force seems to act between their frequencies as clearly seen around 30 GPa. A very similar behavior is successively seen along an extrapolated decreasing curve of the $\nu_{1,3}$ frequency around 40 GPa with the $2\nu_{R'}$ frequency and around 45 GPa with the $2\nu_R$ frequency. The ν_2 frequency is insensitive to pressure, staying at 1600 cm^{-1} up to 40 GPa. Along the flat frequency-pressure line, an avoided crossing in frequency is found to take place at about 6 GPa and again at about 22 GPa, although they are small in magnitude compared to those of the $\nu_{1,3}$ stretching modes. These particular behaviors are also observed for D_2O ice, being interpreted in terms of vibrational mode coupling or Fermi resonance.

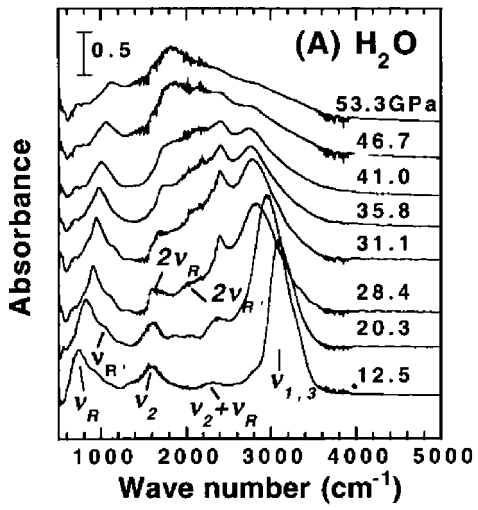

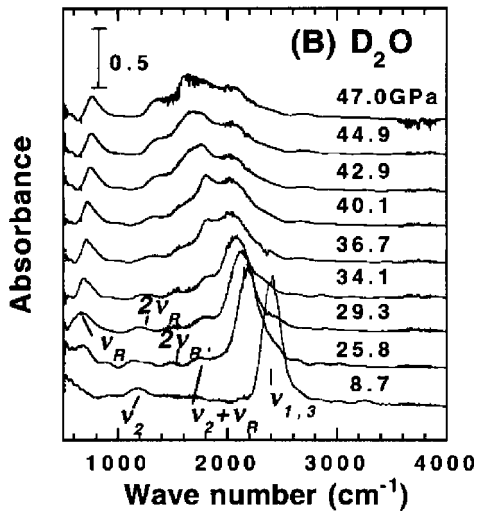

FIG. 3. Infrared spectra of (A) H_2O and (B) D_2O ice VII at 298 K and pressure below 54 GPa. All these spectra are measured using a DAC with 1.5-mm diamond anvils. The $\nu_{1,3}$ stretching peaks move to low frequency, showing sequential Fermi resonance with the $\nu_2+\nu_R$, $2\nu_{R'}$, and $2\nu_R$ peaks (see also Fig. 4). The CO_2 peaks involved in the original spectra at 2300–2400 cm^{-1} have artificially been removed.

The $\nu_{1,3}$ stretching frequency is largely modified as the result of mode mixing or Fermi resonance successively induced with increasing pressure as shown in Fig. 4. The low-pressure frequencies below 20 GPa in H_2O and below 30 GPa in D_2O are well described with a phenomenological function, $\nu_{OH}=(\nu_0^2-aP)^{1/2}$.[5] The *softening* behavior is perturbed by the mode mixing effect and consequently an expected decrease in frequency toward zero cannot be seen in a higher pressure region above 20 GPa. However, the unperturbed or bare frequencies are able to be estimated by analyzing the resonanced spectra under some assumptions; the bare frequencies of the stretching modes are described with a function $\nu_{OH}=(\nu_0^2-aP)^{1/2}$ just mentioned above, while those of the other modes with second-order polynomials of pressure. The analysis based on the simplified classical mechanical model would be available for the low-pressure data measured roughly below 40 GPa. To analyze the observed frequencies especially of the $\nu_{1,3}$ stretching modes, a

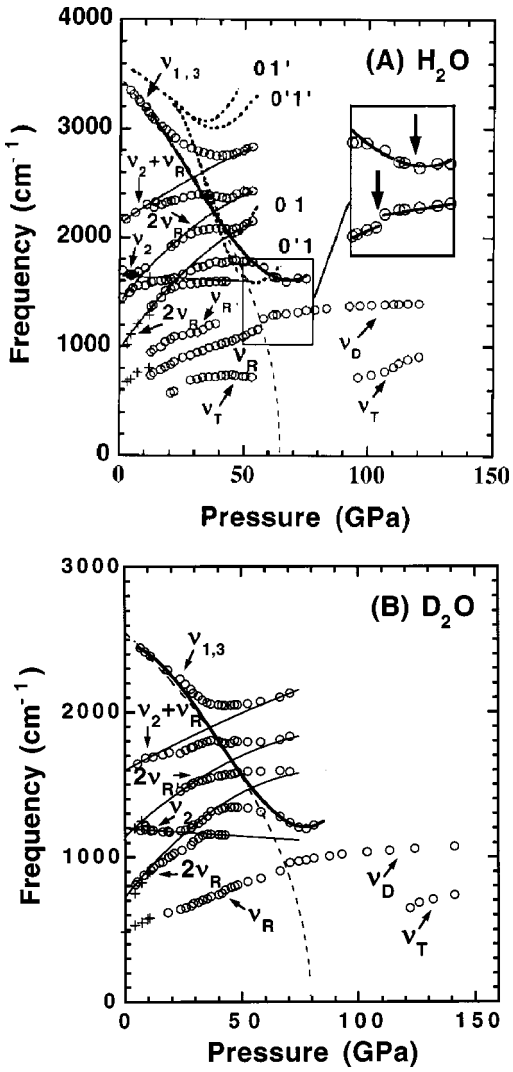

FIG. 4. Pressure variation of the vibrational frequencies for (A) H_2O up to 120 GPa and (B) D_2O up to 141 GPa at 298 K. Open circles: the present IR data; crosses: the IR data from Ref. 22; fine solid lines: the speculated bare frequencies; a broken line: a fitted stretching frequencies based on a classical harmonic model. The stretching frequencies calculated for H_2O ice based on a quantum-mechanical model are also drawn with dotted lines in (A), where $0'1$, 01, $0'1'$, and $01'$ stand for $^*E_{0'} \rightarrow {}^*E_1$, $^*E_0 \rightarrow {}^*E_1$, $^*E_{0'} \rightarrow {}^*E_{1'}$, and $^*E_0 \rightarrow {}^*E_{1'}$ excitation, respectively, between the tunnel splitting levels (see the text and Ref. 19).

quantum-mechanical treatment of the proton vibrational states should be taken into account as discussed in detail later. Nevertheless, the classical analysis is an effective method to obtain an approximate perspective for the influence of pressure on the vibrational states including the softening behavior of the stretching modes.

A method equivalent to a harmonic approximation has been applied to the analysis of Fermi resonance in H_2O ice.[16] The coupling parameters between the resonanced vibrational modes can be obtained by solving a secular equation for the vibrational frequencies modified by interaction Δ_{nk},

$$|(-\omega^2+\Omega^2{}_k)\,\delta_{nk}+\Delta_{nk}{}^2|=0, \tag{1}$$

where the index n is the number of vibrational modes, k is the integer from 1 to n, ω and Ω_k are the observed and bare

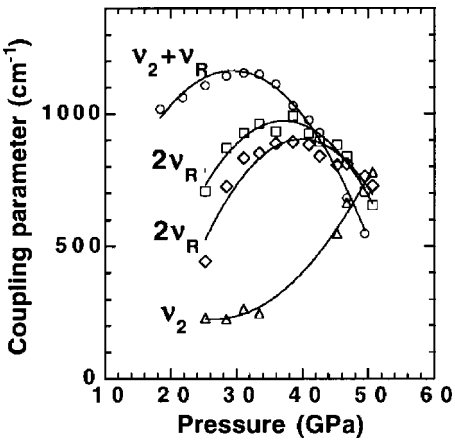

FIG. 5. Pressure variation of the coupling parameters of Fermi resonance of the $\nu_2+\nu_R$, $2\nu_{R'}$, $2\nu_R$, and ν_2 modes with the $\nu_{1,3}$ soft mode in H_2O ice. Solid lines are the guides to the eye.

frequencies, respectively, and Δ_{nk} is a coupling parameter. Using the observed and assumed bare frequencies at each pressure, we can solve this determinant to get the coupling parameter Δ_{nk}.

The parameters obtained for H_2O ice are given in Fig. 5. The coupling parameters of the $\nu_{1,3}$ soft mode with the $\nu_2+\nu_R$, $2\nu_{R'}$ and $2\nu_R$ modes show similar pressure dependence; they increase initially with pressure and turn to decrease after reaching the maximum points. We can reasonably take a pressure at the maximum point as an exactly resonanced pressure for each resonance: 28 GPa with the $2\nu_{R'}$ mode, 35 GPa with the $2\nu_{R'}$ mode, and 40 GPa with the $2\nu_R$ mode. In contrast to these resonances, the resonance between the $\nu_{1,3}$ and ν_2 modes exhibits a different pressure behavior. The coupling parameter increases monotonically from about 200 cm^{-1} at around 20 GPa to 800 cm^{-1} at about 50 GPa, showing no maximum in the pressure span measured. We performed the analysis for the D_2O data. The resonance parameter between the $\nu_{1,3}$ and $\nu_2+\nu_R$ is about 800 cm^{-1} smaller by 400 cm^{-1} than that of H_2O ice at the maximum point. In addition to the coupling parameters, the resonance analysis also yields the bare frequencies. They are drawn by a broken line for the $\nu_{1,3}$ stretching mode and by fine solid lines for the other modes in Figs. 4(A) and 4(B).

C. Hydrogen-bond symmetrization

The spectra of H_2O and D_2O ices measured beyond 55 GPa with the thick diamond anvils are shown in Figs. 6(A) and 6(B). The spectrum of H_2O at 57.9 GPa is featureless, showing two broad peaks with the peak tops around 1250 and 1750 cm^{-1}. On further compression, the absorption peak located at 1250 cm^{-1} develops into a sharp and intense peak. Another peak, which has likely been moving to high frequency with pressure, exhibits its whole peak shape around 900 cm^{-1} eventually. The spectrum at 120 GPa shows two peaks alone at about 900 and 1400 cm^{-1}. This spectral feature is entirely different from that observed for the low-pressure spectrum of ice VII, suggesting a phase transition from phase VII to a higher symmetry structure while the pressure increases up to 120 GPa. A very similar change is seen in the spectra measured for D_2O ice as shown in Fig.

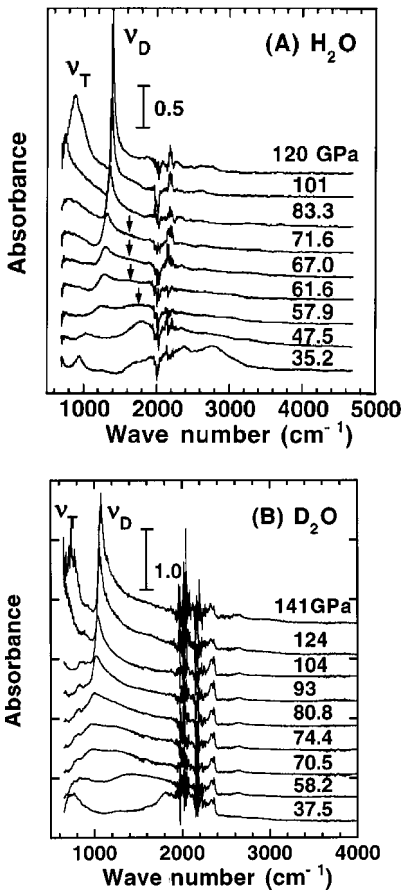

FIG. 6. IR spectra of (A) H_2O ice up to 120 GPa and (B) D_2O ice up to 141 GPa at 298 K. The peak located at 1250 cm^{-1} in the H_2O spectrum at 57.9 GPa grows to a sharp peak with increasing pressure. Another peak appears at 900 cm^{-1} in a 120-GPa spectrum. The low-and high-frequency peaks are assigned as the translation lattice mode ν_T and distortional lattice mode ν_D of the symmetrized hydrogen bond phase. A similar spectral change is seen in the D_2O spectra. The peaks at 750 and 1050 cm^{-1} in a 141-GPa spectrum are assigned as the ν_T and ν_D modes, respectively. The noises in a region 1800–2400 cm^{-1} arise from incomplete cancellation of the diamond absorption.

6(B). Two peaks located at about 750 and 1050 cm^{-1} at 141 GPa correspond to those in the 120–GPa spectrum of H_2O ice.

The observed spectral changes are well interpreted in terms of a phase transition from molecular phase VII to symmetric phase X. Symmetric ice X is speculated to possess a cuprite Cu_2O structure. Oxygen atoms form a bcc lattice with hydrogen atoms at the midpoints between the neighboring oxygen atoms. The hydrogen atoms hence construct a tetrahedron with one oxygen atom at the center. A vibrational mode analysis has predicted two IR-active lattice modes for the symmetric ice with a cuprite Cu_2O structure: a distortional twisting of the tetrahedron of hydrogen atoms around a resting oxygen atom, ν_D, and a translational motion of oxygen and hydrogen atoms in the opposite direction, ν_T.[25] The spectra of H_2O ice above 101 GPa and D_2O ice above 124 GPa with two IR absorption peaks alone are exactly in agreement with the vibrational mode analysis, providing clear evidence for the transition into symmetric ice X. The high- and low-frequency peaks can be assigned as the ν_D distortional and ν_T translational mode, respectively. The frequency ratios of $\nu(H_2O)/\nu(D_2O)$ at a corresponding pressure of 120 GPa are very close to 1.41 derived from $(m_H/m_D)^{1/2}$, exhibiting a harmonic isotope behavior of the ν_D and ν_T modes.

Disordered phase VII has theoretically been predicted to appear prior to the transition into disordered phase X.[18] A transition to such a phase, however, is not immediately recognized from the observed spectra; the spectrum changes gradually into that of symmetric phase X above 100 GPa as shown in Fig. 6. A careful investigation on the frequency variations in Fig. 4(A) reveals that the ν_R frequency provides a signal probably related to a transition from phase VII to disordered phase VII. In H_2O ice, an abrupt change in the ν_R frequency is found at about 58 GPa, the frequency increases by about 100 cm^{-1} and becomes less sensitive to pressure above it. We should recall here that the ν_R molecular rotational mode is converted into the ν_D distortional mode in association with the hydrogen bond symmetrization.[26] The changes in the frequency-pressure relation are hence interpreted in terms of the conversion from the ν_R to ν_D mode and consequently from phase VII to disordered phase VII. A similar change is found also in D_2O ice at about 68 GPa, being again explained as a transition into disordered phase VII. A large isotope effect is expected for the VII–disordered-VII transition as the result of the mass effects on zero-point energy and tunneling probability. The present IR measurement provided a pressure difference of about 10 GPa between H_2O and D_2O ices.

We attempt to derive an insight into a further phase transition from disordered VII to disordered X. The ν_D peak of disordered phase VII of H_2O ice shows an asymmetric shape with a long tail extending well up to 3000 cm^{-1} as shown in Fig. 6(A). In a 61.6-GPa spectrum, we can scarcely see an additional peak (indicated by arrows) on the tail around 1600 cm^{-1}. This peak, which originates from the molecular stretching vibration, gradually disappears at about 75 GPa likely associated with the disordered-VII–disordered-X transition as discussed in the following paragraphs.

The proton vibrational states in the hydrogen bonding potential changing from a double to single minimum shape have precisely been calculated on the basis of a quantum-mechanical model including proton tunneling.[19] Each vibrational energy level of the proton originally localized at one minimum will split into a doublet when the midpoint barrier top, which is depressed continuously to zero by compression, approaches and passes through it. An energy splitting hence occurs successively with increasing pressure from a higher energy level, for instance, as $E_2 \rightarrow {}^*E_{2,2'}$, $E_1 \rightarrow {}^*E_{1,1'}$ and finally $E_0 \rightarrow {}^*E_{0,0'}$, where E_n and ${}^*E_{n,n'}$ represent the energies of the singlet and doublet states, respectively. The observed stretching frequencies at low pressures below 20 GPa corresponds to an $E_0 \rightarrow E_1$ excitation of the proton trapped in one minimum, being converted gradually into an $E_0 \rightarrow {}^*E_1$ excitation just before the VII–disordered-VII transition and eventually into an ${}^*E_{0'} \rightarrow {}^*E_1$ excitation after it. The stretching frequencies thus calculated for H_2O ice are drawn by dotted lines in Fig. 4(A), showing a decrease with pressure to 1600 cm^{-1} at about 58 GPa and a slight increase on further compression.

The bare stretching frequency is found to trace the frequency-pressure curve calculated based on a quantum-mechanical model. Although the $\nu_{1,3}$ stretching frequencies observed were perturbed by Fermi resonance, the analysis of the resonanced vibrational states provided the unperturbed frequencies for the pressure range below 40 GPa for H_2O ice and below 50 GPa for D_2O ice. The bare stretching frequencies obtained for H_2O ice are shown to connect continuously and smoothly to a frequency minimum located at 1600 cm^{-1} and about 67 GPa very close to the location of the calculated minimum. The essential feature of the frequency-pressure curve thus drawn is well in agreement with that theoretically calculated [compare the solid line and the dotted $0'1$ line in Fig. 4(A)]. A minimum in the frequency is located at 67 GPa just above 58 GPa, where the VII–disordered-VII transition takes place. This is also predicted from the calculation.[19] In the spectra of D_2O ice, a frequency minimum can be seen at about 80 GPa just above the VII to disordered VII transition pressure of 68 GPa as well [Fig. 4(B)].

The energy-level calculation leads to a further plausible interpretation of the IR spectra that the disappearance of the 1600-cm^{-1} peak of H_2O ice provides roughly an estimation for the transition pressure from disordered VII to disordered X. An increase in the ground-state splitting $^*E_0 - {}^*E_{0'}$ with pressure, will reduce the population of the first excitation level at $^*E_{0'}$ and consequently the transition probability associated with the $^*E_{0'} \rightarrow {}^*E_1$ excitation. The population thermally activated to the $^*E_{0'}$ state (the initial state of the $^*E_{0'} \rightarrow {}^*E_1$ excitation) should become small for a sufficiently widened $^*E_0 - {}^*E_{0'}$ splitting, which may induce relocation of the proton to the midpoint of the hydrogen bonds, that is, a transition into disordered phase X; the calculation predicted a splitting of 500 cm^{-1} or 700 K at the transition point.[6] The peak disappearance can therefore be considered as a signal of a transition from disordered phase VII to disordered X with a unimodal proton distribution. The transition pressures thus estimated are 65–75 and 80–90 GPa for H_2O and D_2O ices, respectively.

Finally, we compare the results of the present IR measurement with those obtained by the x-ray diffraction on ice. Powder-diffraction measurements have been made for H_2O ice up to 128 GPa.[3,9] They showed the presence of the bcc sublattice of oxygen atoms for the whole pressure region measured above 2 GPa, indicating that the hydrogen bond symmetrization is realized in the bcc lattice at a certain threshold pressure. The observed equation of state provided a signature of phase transition at about 66–70 GPa,[8,9] close to the disordered-VII–disordered-X transition pressure of 65–75 GPa roughly estimated from the IR spectra. Very recently a more direct measurement on the proton centering in ice was carried out by single-crystal x-ray-diffraction measurement.[27] The intensity change in diffraction from the proton sublattice indicated a proton centering at about 60 GPa again close to those determined by the IR spectra. This change, however, should be interpreted as a transition from phase VII to phase X without passing through the intermediate disordered phase VII. Another run of the same single-crystal diffraction measurement revealed that the proton centering occurred at about 40 GPa far below 60 GPa. The IR spectra measured around this pressure exhibited clearly the spectral features due to H_2O molecular vibrations, showing no evidence for a transition into phase X. The phase identification still remains inconclusive between the IR absorption and x-ray-diffraction measurements.

ACKNOWLEDGMENT

This work was conducted under the Core Research for Evolutional Science and Technology (CREST) project supported by Japan Science and Technology Corporation (JST).

*Author to whom correspondence should be addressed.

[1] W. F. Kuhs, J. L. Finney, C. Vettier, and D. V. Bliss, J. Chem. Phys. **81**, 3612 (1984).
[2] J. D. Jorgensen and T. G. Worlton, J. Chem. Phys. **83**, 329 (1985).
[3] R. J. Hemley, A. P. Jephcoat, H. K. Mao, C. S. Zha, L. W. Finger, and D. E. Cox, Nature (London) **330**, 737 (1987).
[4] W. B. Holzapfel, J. Chem. Phys. **56**, 712 (1971).
[5] Ph. Pruzan, J. Mol. Struct. **322**, 279 (1994).
[6] K. Schweizer and F. H. Stillinger, J. Chem. Phys. **80**, 1230 (1984).
[7] C. Lee, D. Vanderbilt, K. Laasonen, R. Car, and M. Parrinello, Phys. Rev. Lett. **69**, 462 (1992).
[8] J. Hama and K. Suito, Phys. Lett. A **187**, 346 (1994).
[9] E. Wolanin, Ph. Pruzan, J. C. Chervin, B. Canny, M. Gauthier, D. Hausermann, and M. Hanfland, Phys. Rev. B **56**, 5781 (1997).
[10] R. J. Nelmes, J. S. Loveday, R. M. Wilson, J. M. Besson, Ph. Pruzan, S. Klotz, G. Hamel, and S. Hull, Phys. Rev. Lett. **71**, 1192 (1993).
[11] J. M. Besson, Ph. Pruzan, and S. Klotz, Phys. Rev. B **49**, 12 540 (1994).
[12] R. J. Nelmes, J. S. Loveday, and W. G. Marshall, Phys. Rev. Lett. **81**, 2719 (1998).
[13] K. Aoki, H. Yamawaki, M. Sakashita, and H. Fujihisa, Phys. Rev. B **54**, 15 673 (1996).
[14] A. F. Goncharov, V. V. Struskin, M. S. Somayazulu, R. J. Hemley, and H. K. Mao, Science **273**, 218 (1996).
[15] K. Aoki, H. Yamawaki, and M. Sakashita, Science **268**, 1322 (1995).
[16] V. V. Struskin, A. F. Goncharov, R. J. Hemley, and H. K. Mao, Phys. Rev. Lett. **78**, 4446 (1997).
[17] C. F. Larsen and Q. Williams, Phys. Rev. B **58**, 8306 (1998).
[18] M. Benoit, D. Marx, and M. Parrinello, Nature (London) **392**, 258 (1998).
[19] P. G. Johannsen, J. Phys.: Condens. Matter **10**, 2241 (1998).
[20] M. Bernasconi, P. L. Silvestrelli, and M. Parrinello, Phys. Rev. Lett. **81**, 1235 (1998).
[21] H. K. Mao, J. Xu, and P. M. Bell, J. Geophys. Res. **91**, 4673 (1986).
[22] W. B. Holzapfel, B. Seiler, and M. Nicol, J. Geophys. Res. **89**, B707 Suppl. (1984).
[23] E. Whalley, Can. J. Chem. **55**, 3429 (1977).
[24] S. P. Tay, D. D. Klug, and E. Whalley, J. Chem. Phys. **83**, 2708 (1985).
[25] K. Huang, Z. Phys. **171**, 213 (1963).
[26] K. R. Hirsch and W. B. Holzapfel, J. Chem. Phys. **84**, 2771 (1986).
[27] P. Loubeyre, R. LeToullec, E. Wolanin, M. Hanfland, and D. Hausermann, Nature (London) **397**, 503 (1999).